Deep-core photoabsorption and photofragmentation of tetrachloromethane near the Cl K-edge

W. C. Stolte, , A. C. F. Santos, , G. G. B. de Souza, , M. M. Sant'Anna, and , and K. T. Leung

Citation: The Journal of Chemical Physics **146**, 214306 (2017); doi: 10.1063/1.4984928
View online: http://dx.doi.org/10.1063/1.4984928
View Table of Contents: http://aip.scitation.org/toc/jcp/146/21
Published by the American Institute of Physics

Deep-core photoabsorption and photofragmentation of tetrachloromethane near the Cl *K*-edge

W. C. Stolte,[1,2,a)] A. C. F. Santos,[3] G. G. B. de Souza,[4] M. M. Sant'Anna,[3] and K. T. Leung[5]
[1]*Department of Chemistry, University of Nevada, Las Vegas, Nevada 89154-4003, USA*
[2]*Advanced Light Source, Lawrence Berkeley National Laboratory, Berkeley, California 94720, USA*
[3]*Instituto de Física, Universidade Federal do Rio de Janeiro, Caixa Postal 68525, 21941-972 Rio de Janeiro, RJ, Brazil*
[4]*Instituto de Química, Universidade Federal do Rio de Janeiro, 21949-900 Rio de Janeiro, RJ, Brazil*
[5]*Department of Chemistry, University of Waterloo, Waterloo, Ontario N2L 3G1, Canada*

(Received 27 February 2017; accepted 19 May 2017; published online 7 June 2017)

The fragmentation of the tetrachloromethane molecule following core-shell photoexcitation and photoionization in the neighborhood of the chlorine *K*-edge has been studied by using time-of-flight mass spectroscopy and monochromatic synchrotron radiation. Branching ratios for ionic dissociation were derived for all the detected ions, which are informative of the decay dynamics and photofragmentation patterns of the core-excited species. In addition, the absorption yield has been measured with a new assignment of the spectral features. The structure that appears above the Cl 1*s* ionization potential in the photoionization spectrum has been ascribed to the existing connection with electron-CCl_4 scattering through experimental data and calculations for low-energy electron-molecule cross sections. In addition, the production of the doubly ionized Cl fragment, Cl^{2+}, as a function of the photon energy has been analysed in the terms of a simple and an appealing physical picture, the half-collision model. *Published by AIP Publishing.* [http://dx.doi.org/10.1063/1.4984928]

I. INTRODUCTION

Absorption of a tender x-ray photon (2-5 keV) by a target may lead to the transfer of an electron from a deep core to an empty orbital or to its ionization. The photoexcited or photoionized molecules with holes in their deep-core shells are substantially unstable and short-lived (about 1 fs or few hundreds of attoseconds). These inner-shell excited states decay by ejecting a photon (fluorescence), one or more electrons (Auger cascades), giving rise to multiply charged moieties, which fragment in a very short time scale.[1]

One photon removes no more than one electron from the molecule. Notwithstanding, eventually two electrons can be ejected though the incident photon interacts with merely one electron in the molecule. This is possible due to the electron-electron interaction via the so-called knock-out (KO) and shake-off (SO) mechanisms.[2,3] Thus, the ejection of two or more electrons from the target is a suitable probe for studying the electron correlation. For atomic targets and for valence and shallow core excitations, the ejection of two or more electrons has small probabilities compared to the single-photoionization process and is, in general, a few percent.[4,5] The same is not true for deep-core excitation, where the multiply charged ions can be formed with significant probabilities. Additionally, two or more electrons can be ejected via the Auger decay after producing a core hole. It can also be more complicated, involving not only a core electron but also valence electrons.[6] As the photon energy increases, the ratio of multiply to singly ionized ions usually also increases up to a maximum from where it gradually decreases towards the so-called shake-off (SO) limit. For excess energies of no more than a few 100 eV, the double ionization process can be ascribed to an internal collision [the so-called knock-out (KO) mechanism]. The photoelectron can interact with the second electron during its way out of the target producing two ejected electrons. The double photoionization process should therefore be similar to the electron impact by the photoelectron that leaves the atom at a low speed. Thus, the ratio of the double to single ionization at low excess energies above the ionization potential, which is the probability for ionization of the second electron, should be proportional to the single electron-impact ionization cross section of the singly charged moiety.[7]

Another scope of this paper is to discuss the shape resonance (SR) observed above the Cl 1s threshold in the CCl_4 molecule. The SR is a continuum resonant process that can be observed in the small molecules.[8,9] It ordinarily appears, within a few eV above an ionization potential, as a broad continuum structure in the photoabsorption and photoionization spectra. The molecular SR can be attributed to the trapping of the photoelectron by a potential barrier through which the electron sooner or later tunnels and is ejected.[9] In this qualitative sketch, the details of the molecular potential play a paramount role due to the roles of the attractive and repulsive parts of the potential resulting from the respective Coulombic and centrifugal forces. This interplay between attractive and repulsive forces controls the shape of the potential. Another picture connects to the chemical features of shape resonances, associating them to empty molecular orbitals close to the continuum. There are important parallels between the both pictures which have been pointed out.[9] The connection between

[a)]Present address: National Security Technologies, LLC, Livermore, CA 94551, USA.

electron-molecule scattering and molecular photoionization, with emphasis on SR's, has been suggested by Dehmer and Dill.[10] They observed that although electron-molecule scattering and molecular photoionization have different electron numbers, the short-range nature of the shape resonances preserves the similarity, even having the long-range part of the potential substantially altered. Of course, a word of caution is in need when applying the half-collision model to shape resonances. Contrary to the case of neutral molecular targets, the potential seen by the ejected electron is no longer a non-Coulombic molecular potential. Moreover, there is not a simple description of the electron angular momentum such as the case of a free electron pictured by a partial-wave expansion. In this paper, we present a model where the photo-excited core-shell electron behaves as a projectile and the residual ionic molecule as a target in an electron attachment collision.

Carbon tetrachloride, also known as tetrachloromethane or CCl_4, is a tetrahedral molecule in its ground state and has been the subject of study for a long time due to its technological applications as an etchant gas in microelectronics.[11,12] The previously measured spectra for inner-shell photoabsorption of CCl_4[13–16] were restricted to the region of Cl 2*p*. Zhang *et al.*[17] reported absolute dipole differential oscillator strengths for Cl *K*-shell spectra from high-resolution electron energy loss studies of CCl_4 among other molecules. Carbon tetrachloride is a closed-shell molecule belonging, in its ground state, to the symmetry point T_d. In an independent particle approximation, its electronic structure is the following:

$$\underbrace{(1a_1)^2(1t_2)^6}_{\text{Cl 1s}} \quad \underbrace{(2a_1)^2}_{\text{C 1s}} \quad \underbrace{(3a_1)^2(2t_2)^6}_{\text{Cl 2s}},$$

$$\underbrace{(4a_1)^2(3t_2)^6(1t_1)^6(1e)^4(4t_2)^6}_{\text{Cl 2p}},$$

$$\underbrace{(5a_1)^2(5t_2)^6(6a_1)^2(6t_2)^6(2e)^4(7t_2)^6(2t_1)^6}_{\text{valence orbitals}},$$

where $(7a_1)^0$ and $(8t_2)^0$ are the lowest unoccupied molecular orbitals (LUMOs).

II. EXPERIMENTAL TECHNIQUE

The measurements were performed on bending magnet beamline 9.3.1 at the Advanced Light Source (Lawrence Berkeley National Laboratory, Berkeley, CA, USA). Calibration at the Cl 1*s*-edge was performed by comparison to the work of Perera *et al.*[18] using the Cl $(1s)^{-1}$ $11a_1$ transition in CF_3Cl at 2823.5 eV. The energy resolution of the photon beam was 0.5 eV.[19] The presented branching ratios were measured with a time-of-flight (TOF) mass spectrometer operated in the space focusing mode,[20] under conditions similar to our previous experimental setup.[21] The total distance traveled by the ions was about 8 cm. The first stage of the electric field consists of a plate-grid system with the light beam passing through its middle part with a 2200 V/cm electric field. The gas inlet needle was kept at ground potential, and the drift tube was kept at 3700 V. The heavier ions required several 328 ns time periods to arrive at the detector, whereas hydrogen arrived in approximately 210 ns. In addition, to keep a constant efficiency for all of the different ionic species, the ions were also required to have sufficient energy such that they strike the front surface of the microchannel plate (MCP) with an energy between 4 and 5 keV. The output pulses from the MCP were fed into conventional electronic counting equipment, with constant fraction discriminators being used to help minimize any electronic noise. In all cases the discrimination level was kept as low as possible, with the levels being verified by comparing the branching ratios for the fragments on resonance while varying the discriminator setting. The target chamber base pressure was in the high 10^{-9} Torr range. In order to minimize the contribution from false coincidences, the pressure during measurements was kept in the mid 10^{-6} Torr range. The ion signal was used to start the time-to-amplitude converter (TAC), and during two-bunch operations of the storage ring, a signal from the synchrotron ring provided a reliable stop pulse for the TAC. During multibunch operations, this stop pulse was provided by electrons emitted from the interaction region, collected on a set of MCP's located on the opposite side of the TOF spectrometer. The presented absorption spectrum, I/I_0, (see Fig. 1) was measured using a static gas cell, containing 35 Torr of CCl_4. The cell was closed on both sides with 500 μm thick Si_3N_4 windows of 2 mm diameter, with a path length of 1.56 cm. The gas cell was preceded in the beamline by an aluminized Mylar foil which was used to measure I_0. The absorption signal I was measured with a Si-photodiode (International Radiation Detectors, Inc., model AXUV100), and the currents from both the aluminized Mylar and the Si-diode were monitored with a pair of calibrated Keithley model 6517A electrometers.

The tetrachloromethane was commercially obtained as a 99.9% pure liquid from Sigma Aldrich. The sample was purged of contaminants by performing a minimum of three freeze/thaw cycles while pumping out the excess vapors from the frozen sample with a mechanical pump, and finally introduced into the chamber after thawing by using its vapor pressure at room temperature.

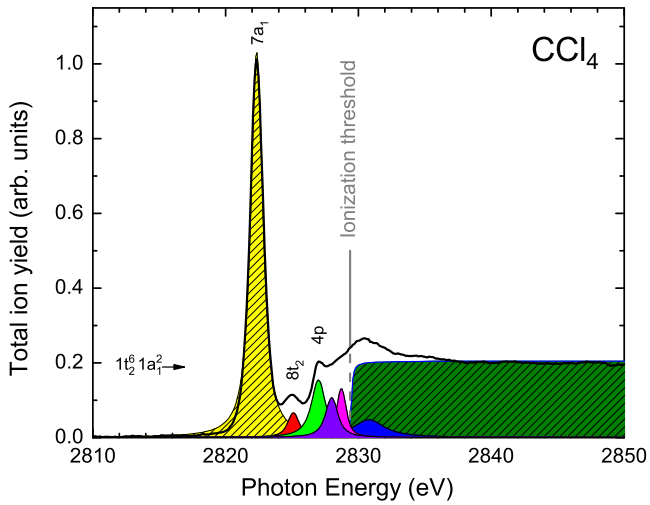

FIG. 1. Total ion-yield spectrum of the CCl_4 molecule near the Cl 1*s* edge. The solid black line represents the measured photoabsorption cross section on a relative scale. The shaded areas represent a multi-peak least squares (Voigt) fit for our experimental data for the 4 below-threshold resonances described in Sec. III A, the first above threshold feature, and a step function to describe the ionization threshold. The grey vertical line corresponds to the Cl 1*s* ionization threshold. Photon energy calibrated to CF_3Cl[18] (see the text).

III. RESULTS

A. Photoabsorption spectra

Figure 1 shows the total ion-yield spectrum of tetrachloromethane near the Cl K-edge. The total ion-yield spectrum mimics the photoabsorption in the present energy range due to the small probability for relaxation through the fluorescence. The main peak in Fig. 1 (2823.4 eV) is the result of Cl 1s resonant excitation $(1t_2)^6(1a_1)^2 \rightarrow 7a_1$. In a previous study, a very similar spectrum was obtained for the related molecule, chloroform or $CHCl_3$, around the Cl K-edge.[22] The colored areas represent a multi-peak least squares fit utilizing Voigt functions for the 4 below-threshold resonances described below, with the Gaussian portion fixed to the known resolution of the beamline. A Gaussian was used to represent the first above threshold feature and a step function (atan) to describe the ionization threshold.

There is a clear structure above the Cl 1s threshold (Fig. 1). We attribute its origin to a shape resonance. This assignment, however, is not straightforward. In a study of L-shell photoionization of CCl_4, Lu *et al.* attributed peaks measured about 1 eV above the Cl $2p_{1/2}$ and Cl $2p_{3/2}$ thresholds to delayed onset and shake-up effects.[12,23] Only a broader structure, about 9 eV above the threshold was assigned by them to a shape resonance. In the absence of theoretical calculations for the Cl 1s photoionization, we seek information using a parallel with experimental data and calculations for low-energy electron-molecule cross sections. This connection, with emphasis on the shape resonances, has been pointed by Dehmer and Dill.[10] They observed that electron-molecule scattering (e^- + M) and molecular photoionization ($h\nu$ + M) systems have different electron numbers. Notwithstanding, they argue that the short-range nature of the shape resonances preserves the similarity, even having the long-range part of the potential substantially altered. Loosely speaking, we picture in the following comparison the photo-excited core-shell electron (in $h\nu$ + M) behaving as a projectile and the residual ionic molecule as a target in an electron attachment collision [a hypothetical e^- + M($1s^{-1}$)].

Braun *et al.* have measured high-resolution electron attachment cross sections for a CCl_4 molecular target.[24] In general, the temporary negative ions are formed and later decay in several channels. The cross sections presented for the Cl_2^- channel show a peak of 1.3 eV above the threshold with a FWHM of 0.6 eV. Jones measured absolute total cross sections for e^- + CCl_4 scattering at low electron energies.[25] In order to interpret the measured structures (see Fig. 2), Jones makes use of calculations using the MS-X method, which provides 4 peaks. Two are interpreted as nonvalence shape resonances of T_2 and E symmetries at 1.74 eV and 6.3 eV, respectively. The other two structures (less intense) are a_1 and e resonances found at 9.4 eV and 13.3 eV, respectively. These assignments are not consensual. Burrow *et al.* measured the low-energy peak at 0.94 eV in an electron transmission spectrum[26] and attributed its origin to a capture of the incident electron in a triply degenerate carbon chlorine antibonding orbital (C–Cl*) of the t_2 symmetry. Curik *et al.* calculated the elastic integral cross sections and discussed the contributions of the A_1, T_2, and E symmetries of the T_d group.[27] In their calculations,

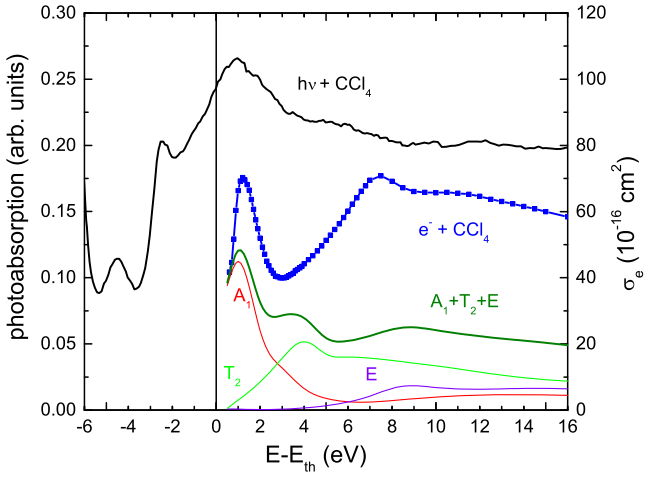

FIG. 2. Photoabsorption of CCl_4 near the Cl 1s edge (photon + CCl_4) as a function of excess energy (photon energy—Cl 1s ionization potential) in comparison to electron scattering on CCl_4. Scale on the left corresponds to the black curve, for all others refer to the left scale.

the lowest energy peak has a dominant A_1 contribution, and the second peak has a dominant T_2 contribution. A contribution of the E symmetry shows two additional maxima. Their results are shown in Fig. 2, together with the experimental data of Jones[25] for total electron scattering cross sections and the present results for photon absorption, as a function of the energy of the projectile minus the threshold energy. Calculations in the static-exchange approximation of Natalense *et al.* also show the three main structures in the A_1, T_2, and E symmetries of the T_d group.[28] Recently, Moreira *et al.* presented calculations based on the Schwinger multichannel method with pseudopotentials and reported two shape resonances at 0.75 eV and 8 eV belonging to the T_2 and E symmetries, respectively.[29] The sum of the contributions from the three symmetries calculated by Curik *et al.*,[27] labeled $A_1 + T_2 + E$ in Fig. 2, shows an energy dependence similar to that of our data (that of course have also a contribution of the direct photoionization channel above the threshold).

In Fig. 3, we show our data for photon absorption and the results for a least squares fit of three Lorentzians, which resulted in an R^2 of 0.996 from the data with an approximate error of 2%. As in Fig. 2, the energy scale is shown in excess energy, which is the photon energy minus the Cl 1s ionization potential for CCl_4. The two first peaks are attributed to the two shape resonances discussed in the aforementioned e^- + CCl_4 studies. With respect to the 1s ionization potential, the most intense peak is located at 1.0 eV and has a linewidth of 3.6 eV. The second most intense peak is located at 5.5 eV and has a linewidth of 3.4 eV. The two peaks marked with ⋆ in Fig. 3 may correspond to the higher energy structures mentioned by Jones[25] at 9.4 eV and 13.3 eV. However, the background in our measurements does not allow unequivocal assignments of these peaks.

B. Ion branching ratios

Ion-yield spectra were taken in the photon energy range of 2802–2872 eV. In Fig. 4, the branching ratios for the most abundant fragments of CCl_4 as a function of the photon energy around the Cl 1s edge is shown. The spectra are dominated

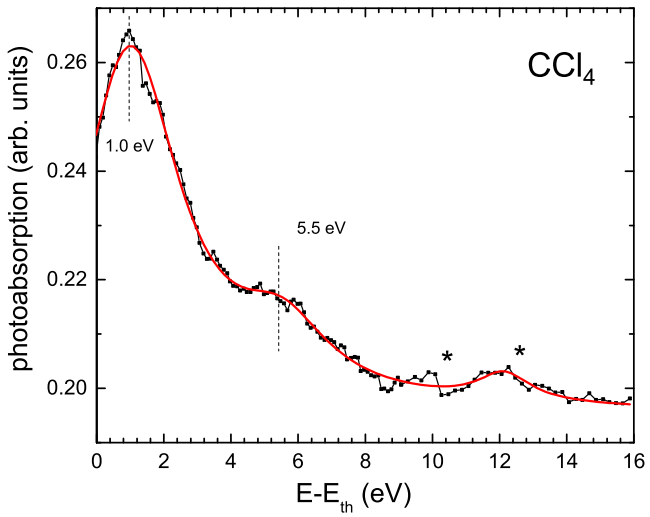

FIG. 3. Data for photon absorption and a simultaneous least squares fit of three Lorentzians versus excess energy. The two first peaks are attributed to the two shape resonances discussed in the e^- + CCl_4 studies.[25,27] ⋆ signifies the locations of higher energy structures mentioned by Jones.[25]

by the Cl^+ fragment, as expected (~75% below the Cl edge and ~52% above the edge). This high probability associated with the Cl^+ fragmentation channel has already been observed above the C 1*s* and Cl 2*p* edges.[14] Its relative intensity shows a local minimum at the $(1t_2)^6(1a_1)^2$ $7a_1$ resonance and a weak local maximum around the $(1t_2)^6(1a_1)^2 8t_2$ and $(1t_2)^6(1a_1)^2$ 4*p* resonances, and it continuously decreases above the Cl 1*s* continuum.

The C^+ branching ratio exhibits a roughly complementary behavior in relation to the Cl^+ ion, indicating a completely different mechanism for creation than that of the singly charged Cl ion. Its relative intensity quickly increases from ~15% above the edge to ~24% at Cl 1*s* continuum. It reaches a maximum at the $(1t_2)^6(1a_1)^2$ $7a_1$ resonance, probably due to the role played by the resonance Auger decay, and a minimum near the $(1t_2)^6(1a_1)^2 8t_2$ resonance. The only molecular fragment observed in the present energy range is the CCl^+ ion (4% below and 1% above the edge), which has a similar appearance to that of the Cl^+ ion. The two doubly-charged fragments, Cl^{2+} and C^{2+}, can be observed with the relevant statistics (0.5%). Both the branching ratios increase nonlinearly as a function of the photon energy. Figure 4 also shows the sum of the corresponding branching ratios for the rest of fragments, which do not reach 0.6%.

We now discuss an analysis of double ionization, above the Cl 1*s* ionization potential, based on the half-collision model.[30,31] Double photoionization can be treated as a sequence of two independent processes. It begins with the photoionization of a single electron. This photoelectron then causes the electron-impact ionization of the remaining system. Our experimental comparison can be seen as an incremental step of the simple picture formally proposed by Samson[7] for the valence shell double ionization of atoms by its application to the inner-shell and molecular systems. The removal of a second electron in the photo-double ionization process should be similar to the electron-impact ionization cross section from any photoelectron leaving the molecule at a low speed. Thus, the ratio of double to single ionization in the low excess energy range (applied photon energy minus the Cl 1*s* ionization potential) is proportional to the probability of photoionization of a second electron from the singly charged ion, which should be proportional to the electron-impact single ionization cross section of that same singly charged ion. By picturing electron-electron scattering, electron correlation in the double-ionization continuum can therefore be understood. There are, nevertheless, significant differences to electron-impact ionization. As the photoelectron (the projectile) is originally localized inside the molecule near the nucleus, the electron correlation on the way out resembles a half-collision. This mechanism is sometimes denoted as a knock-out (KO) or two-step 1 (TS1) process.[5] Additionally, while the electron-impact single ionization cross section decreases as $\ln(v)/v^2$, where v is the electron speed, the double-ionization cross section should come together to the "shake-off" (SO) limit.[4] In the KO empirical model, the double

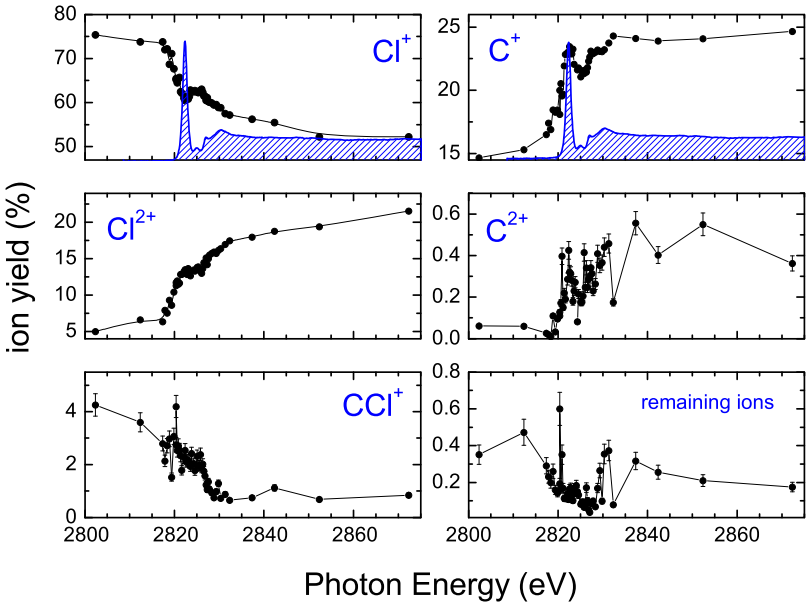

FIG. 4. The partial ion yield of prominent CCl_4 fragments as a function of the photon energy near the Cl 1*s* edge. The total ion-yield spectrum (blue line/area) is also shown for the sake of the visual comparison.

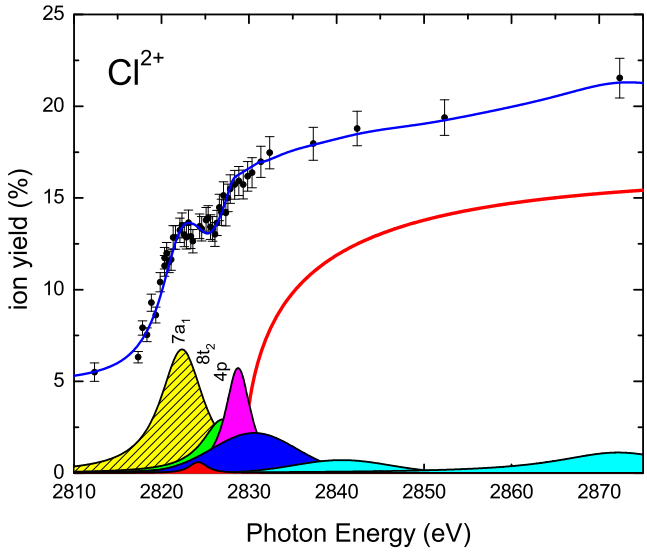

FIG. 5. The Cl^{2+} branching ratio as a function of the photon energy. A set of Voigt functions representing the resonances (see Fig. 1) added to a constant background due to Cl 2*p*, Cl 2*s*, and C 1*s* contributions. Red line: calculated KO model [Eq. (1)].

ionization branching ratio as a function of the photon energy is given by[32]

$$P_{KO}(E) = P_{KO}^{max}\left\{\cosh\left(\beta \ln\left[\frac{E - I_p^{2+}}{\Delta E_{KO}^{max}}\right]\right)\right\}^{\frac{-1}{\beta}}, \qquad (1)$$

where Eq. (1) represents the analytical form of the universal shape function for electron-impact ionization of H-like ions of Aichele *et al.*[33] Figure 5 shows the Cl^{2+} branching ratio as a function of the photon energy. Similar to Fig. 1, a set of Voigt functions representing the various below threshold resonances were added to a constant background due to Cl 2*p*, Cl 2*s*, and C 1*s* contributions. The KO model [Eq. (1)] is shown in the figure above the Cl 1*s* ionization potential as the bold red curve. The blue line represents a sum of all of the before mentioned curves, agreeing with the experimental results.

IV. CONCLUSIONS

We have studied the fragmentation of the CCl_4 molecule, following core-shell photoexcitation and photoionization in the neighborhood of the Cl 1*s* edge. The absorption yield has been ascribed to a new assignment of the spectral features. The structure that appears above the Cl 1*s* continuum has been ascribed to two shape resonances in terms of the existing connection with electron-CCl_4 scattering through experimental data and calculations for the low-energy electron-molecule cross sections. Furthermore, the production of the doubly ionized Cl fragment as a function of the photon energy has been analysed in the terms of a simple and an appealing physical picture, the half-collision model.

ACKNOWLEDGMENTS

This work is supported in part by CNPq, FAPERJ, and CAPES (Brazil). The authors would like to express their gratitude to the staff of the Advanced Light Source (ALS) for their valuable help during the course of the experiments. The Advanced Light Source is supported by DOE (No. DE-AC03-76SF00098). We are particularly indebted to Professor C. Cisneros and Professor A. Schlachter.

[1] O. Travnikova, T. Marchenko, G. Goldsztejn, K. Jnkl, N. Sisourat, S. Carniato, R. Guillemin, L. Journel, D. Colin, R. Pttner, H. Iwayama, E. Shigemasa, M. N. Piancastelli, and M. Simon, Phys. Rev. Lett. **116**, 213001 (2016).
[2] T. Schneider, P. L. Chocian, and J. M. Rost, Phys. Rev. Lett. **89**, 073002 (2002).
[3] T. D. Thomas, Phys. Rev. Lett. **52**, 417 (1984).
[4] A. C. F. Santos and D. P. Almeida, J. Electron Spectrosc. Relat. Phenom. **210**, 1 (2016).
[5] R. D. DuBois, A. C. F. Santos, and S. T. Manson, Phys. Rev. A **90**, 052721 (2014).
[6] M. Q. AlKhaldi and R. Wehlitz, J. Chem. Phys. **144**, 044304 (2016).
[7] J. A. R. Samson, Phys. Rev. Lett. **65**, 2861 (1990).
[8] D. Dill, J. R. Swanson, S. Wallace, and J. L. Dehmer, Phys. Rev. Lett. **45**, 1393 (1980).
[9] M. N. Piancastelli, J. Electron Spectrosc. Relat. Phenom. **100**, 167 (1999).
[10] J. L. Dehmer and D. Dill, in *Shape-Resonance-Enhanced Nuclear Motion Effects in Electron-Molecule Scattering and Molecular Photoionization*, edited by N. Oda and K. Takavanagi (North-Holland, Amsterdam, The Netherlands, 1980), p. 858, ISBN: 0 444 85434 7; J. L. Dehmer and D. Dill, in *International Conference on the Physics of Electronic and Atomic Collisions* (North-Holland Pub. Co., New York, 1980), Vol. 11, pp. 195–208.
[11] G. C. Schwartz and P. M. Schaible, J. Vac. Sci. Technol. **16**, 410 (1979).
[12] K. T. Lu, J. M. Chen, J. M. Lee, C. K. Chen, T. L. Chou, and H. C. Chen, New J. Phys. **10**, 053009 (2008).
[13] M. de Simone, M. Coreno, M. Alagia, R. Richter, and K. C. Prince, J. Phys. B: At., Mol. Opt. Phys. **35**, 61 (2002).
[14] A. C. F. Santos, J. B. Maciel, and G. G. B. de Souza, J. Electron Spectrosc. Relat. Phenom. **156-158**, 236 (2007).
[15] B. E. Cole and R. N. Dexter, J. Quant. Spectrosc. Radiat. Transfer **19**, 303 (1978).
[16] G. O'Sullivan, J. Phys. B: At., Mol. Opt. Phys. **15**, 2385 (1982).
[17] W. Zhang, T. Ibuki, and C. E. Brion, Chem. Phys. **160**, 435 (1992).
[18] R. C. C. Perera, P. L. Cowan, D. W. Lindle, R. E. LaVilla, T. Jach, and R. D. Deslattes, Phys. Rev. A **43**, 3609 (1991).
[19] M. Simon, L. Journel, R. Guillemin, W. C. Stolte, I. Minkov, F. Gel'mukhanov, P. Sałek, H. Ågren, S. Carniato, R. Taïeb, A. C. Hudson, and D. W. Lindle, J. Electron Spectrosc. Relat. Phenom. **155**, 91 (2007).
[20] W. C. Wiley and I. H. McLaren, Rev. Sci. Instrum. **26**, 1150 (1955).
[21] J. A. R. Samson, W. C. Stolte, Z.-X. He, J. N. Cutler, Y. Lu, and R. J. Bartlett, Phys. Rev. A **57**, 1906 (1998).
[22] A. F. Lago, A. C. F. Santos, W. C. Stolte, A. S. Schlachter, and G. G. B. de Souza, J. Electron Spectrosc. Relat. Phenom. **144-147**, 161 (2005).
[23] K. T. Lu, J. M. Chen, J. M. Lee, S. C. Haw, T. L. Chou, S. A. Chen, and T. H. Chen, Phys. Rev. A **80**, 033406 (2009).
[24] M. Braun, S. Marienfeld, M.-W. Ruf, and H. Hotop, J. Phys. B: At., Mol. Opt. Phys. **42**, 125202 (2009).
[25] R. K. Jones, J. Chem. Phys. **84**, 813 (1986).
[26] P. D. Burrow, A. Modelli, N. S. Chiu, and K. D. Jordan, J. Chem. Phys. **77**, 2699 (1982).
[27] R. Curik, F.A. Gianturco, and N. Sann, J. Phys. B: At., Mol. Opt. Phys. **33**, 615 (2000).
[28] A. P. P. Natalense, M. H. F. Bettega, L. G. Ferreira, and M. A. P. Lima, Phys. Rev. A **52**, R1 (1995).
[29] G. M. Moreira, A. S. Barbosa, D. F. Pastega, and M. H. F. Bettega, J. Phys. B: At., Mol. Opt. Phys. **49**, 035202 (2006).
[30] T. Pattard and J. Burgdörfer, Phys. Rev. A **64**, 042720 (2001).
[31] W. C. Stolte, V. Jonauskas, D. W. Lindle, M. M. Sant'Anna, and D. W. Savin, Astrophys. J. **818**, 149 (2016).
[32] J. Hoszowska, J.-Cl. Dousse, W. Cao, K. Fennane, Y. Kayser, and M. Szlachetko, Phys. Rev. A **82**, 063408 (2010).
[33] K. Aichele, U. Hartenfeller, D. Hathiramani, G. Hofmann, V. Schfer, M. Steidl, M. Stenke, E. Salzborn, T. Pattard, and J. M. Rost, J. Phys. B: At., Mol. Opt. Phys. **31**, 2369 (1998).